Pergamon

Geochimica et Cosmochimica Acta, Vol. 67, No. 7, pp. 1415–1427, 2003

0016-7037/03 $30.00 + .00

doi:10.1016/S0016-7037(02)01181-X

# Alkali exchange equilibria between a silicate melt and coexisting magmatic volatile phase: An experimental study at 800°C and 100 MPa

MARK R. FRANK,* PHILIP A. CANDELA, and PHILIP M. PICCOLI

Laboratory for Mineral Deposits Research, Department of Geology, University of Maryland, College Park, MD 20742, USA

(*Received September* 18, 2001; revised 22 July 2002; *accepted in revised form July* 22, 2002)

**Abstract**—Many experimental studies have been performed to evaluate the composition of coexisting silicate melts and magmatic volatile phases (MVP). However, few studies have attempted to define the relationship between melt chemistry and the acidity of a chloride-bearing fluid. Here we report data on melt composition as a function of the HCl concentration of coexisting brines. We performed 35 experimental runs with a NaCl-KCl-HCl-$H_2O$ brine (70 wt% NaCl [equivalent])-silicate melt (starting composition of $Qtz_{0.38}Ab_{0.33}Or_{0.29}$, anhydrous) assemblage at 800°C and 100 MPa. We determined an apparent equilibrium constant

$$K'_{meas}\,(K, Na) = (C^m_{Na} \times C^b_{KCl})/(C^b_{NaCl} \times C^m_K)$$

for the equilibrium

$$NaCl^b + \Sigma K^m = \Sigma Na^m + KCl^b,$$

(where $C^b_{KCl}$, $C^b_{NaCl}$, $C^m_K$, and $C^m_{Na}$ are total concentrations of potassium and sodium chloride in the brine, and potassium and sodium in the melt, respectively) as a function of the HCl concentration in the brine ($C^b_{HCl}$). Although $K'_{meas}$ (K, Na) was not affected by variations in KCl/NaCl of the brine, it did vary inversely with $C^b_{HCl}$. The relationship is given by

$$K'_{meas}\,(K, Na) = K'_{ex}\,(K, Na) + \frac{a}{C^b_{HCl}}$$

[where $C^b_{HCl}$ is in wt% and $a = 0.03$; $K'_{ex}$ (K, Na) = 0.40 ± 0.03 (1$\sigma$) and represents the exchange of model sodium and potassium between chloride components in the brine and the aluminate components ($NaAlO_2$ and $KAlO_2$) in the melt. This empirical result will be discussed in light of a structural hypothesis; however, validation of the model awaits determinations based on spectroscopy or transport properties–thermodynamic relations alone cannot be used as evidence of structure. The form of this equation is consistent with a model wherein sodium is present in the melt as both sodium aluminate and sodium hydroxide components, and HCl reacts with the NaOH component in the melt to produce NaCl and $H_2O$.

The correlation between fugacity of $H_2O$ ($f^{sys}_{H_2O}$), model $NaOH^m/\Sigma Na^m$, aluminum saturation index (ASI), and the ratio $(HCl/NaCl)^b$ of an exsolving MVP is complex. $f^{sys}_{H_2O}$ and the ASI are the main controls on model $NaOH^m/\Sigma Na^m$ in the system, with model $NaOH^m/\Sigma Na^m$ increasing with increasing $f^{sys}_{H_2O}$. This relationship can be used to estimate the $C^b_{HCl}$ in subaluminous systems, an improvement over previous models. Data for metal partitioning between a volatile phase and melt are commonly presented in the literature as metal–sodium exchange equilibria (i.e., $K_{Cu,Na}$ for the exchange of copper and sodium). However, the variation in $K'_{meas}$ (K, Na) observed in this study implies that the treatment of metal partitioning between a volatile phase and melt as metal–alkali exchange equilibria is complex because alkali partitioning is not constant and suggests that experimental partitioning studies need to carefully control the HCl/NaCl in experimental vapors and brines. This effect may explain discrepancies in metal–alkali exchange equilibria presented in the literature. Therefore, metal–alkali exchange cannot be described fully by a single metal–alkali equilibrium but must be examined by multiple equilibria. 

## 1. INTRODUCTION

Some magmatic processes, such as volcanic eruptions, differentiation of silicate melts, and the genesis of magmatic–hydrothermal ore deposits, are controlled in part by the interaction between silicate and dissolved volatile components in silicate melts. Many workers have studied the exchange of components between a silicate melt and magmatic volatile phase (MVP) over a range of temperatures, pressures, and compositions (Gammon et al., 1969; Holland, 1972; Shinohara, 1987; Webster and Holloway, 1988; Webster et al., 1989; Candela, 1990; Williams et al., 1997; Schäfer et al., 1999; Student and Bodnar, 1999). How the composition of the melt, along with temperature, pressure and other intensive variables, control the composition of the MVP and the amount of metals that may be scavenged from the melt and transported to the porphyry or epithermal environment is still not well understood. Before any comprehensive modeling of magmatic–hy-

* Author to whom correspondence should be addressed, at Geophysical Laboratory, Carnegie Institution of Washington, 5251 Broad Branch Road, Washington, DC 20015, USA (m.frank@gl.ciw.edu).

drothermal systems can be performed, the relationship between melt composition and MVP composition must be understood.

In this study, the exchange of components between a silicate melt and coexisting brine (high-salinity liquid phase) was analyzed to determine, in detail, how melt and brine compositions are linked, especially with regard to the affect of melt composition on MVP acidity The acidity of a MVP has been shown to be of major importance for processes in magmatic hydrothermal systems ranging from mineral alteration (Hemley, 1959; Sverjensky et al., 1991; Frank et al., 1998) to hydrothermal ore deposition (Hemley and Hunt, 1992; Gammons and Williams-Jones, 1995; Frank et al., 2002). Yet many experimental studies ignore HCl by excluding it from the starting solution or allowing it to remain unbuffered throughout the experiment. Here we report data from a study that aimed to change geologically reasonable variables (including salinity, KCl/NaCl starting value, and starting HCl concentration) in a thermodynamically systematic manner to study the dynamics of the melt–brine system.

The structure of silicate melts provides a basis for the rationalization of the physicochemical properties needed to describe igneous processes including those that may affect magmatic–hydrothermal systems. This study was designed to obtain compositional data and apply these data to *hypotheses* on melt structure, especially as it bears on issues related to chloride and ore metals; however, it is important to emphasize that whereas thermodynamic arguments can suggest hypotheses for melt structure, the validation of melt structure hypotheses must await spectroscopic or transport property studies. Understanding the genesis of a MVP and the components in silicate melts is necessary to define the mass transfer equilibria that control the partitioning of chloride and chloride-complexed metals between melts and either crystalline phases or volatile phases. The use of the improper equilibria, or worse, simple Nernst-type partition coefficients for chloride, yield the incorrect mass-action effects when modeling devolatilization. Table 1 lists variables and notations used herein.

Table 1. Terminology, variables, and notations.

**Terminology**

| | |
|---|---|
| Brine | high-salinity liquid phase |
| Vapor | low-salinity vapor phase |
| MVP | (magmatic volatile phase) refers to any gas or aqueous chloride-bearing liquid which exsolves from a silicate melt |
| Melt | silicate melt |

**Variables**

| | |
|---|---|
| $C_i^j$ | concentration of component i in phase j (wt%) |
| $X_i^j$ | mole fraction of component i in phase j |
| $D_i^{j/y}$ | Nernst-type partition coefficient for component i between phases j and y |
| $a_i^j$ | activity of component i in phase j ($a_i^j = \gamma_i^j \times C_i^j$) |
| $\gamma_i^j$ | activity coefficient of component i in phase j |
| K (h) | equilibrium constant of equilibrium h at a given temperature and pressure |
| K' (h) | apparent equilibrium constant of equilibrium h at a given temperature and pressure (does not account for activity coefficients) |

**Notation**

| | | | |
|---|---|---|---|
| sys | system | aq | aqueous phase (vapor, brine, or supercritical fluid) |
| b | brine | aqm | aqueous mixture (vapor + brine) |
| v | vapor | scf | supercritical fluid |
| | | fg | final glass |
| m | melt | ig | initial glass |
| g | glass | fap | final aqueous phase |
| o | standard state | iap | initial aqueous phase |

## 2. EXPERIMENTAL AND ANALYTICAL METHODS

### 2.1. Experimental Procedures

Brines were equilibrated with silicate melts at 800°C and 100 MPa. Experiments were conducted in gold capsules with an outer diameter of 5.0 mm, inner diameter of 4.8 mm, and length of 0.20 mm. Approximately 50 mg of powdered synthetic glass and brine starting materials were loaded into each capsule. The starting glass, $Qtz_{0.38}Ab_{0.33}Or_{0.29}$ on an anhydrous basis (Table 2), has the composition of a 100-MPa hydrated minimum melt (with a 100-MPa solidus temperature of ~720°C; Tuttle and Bowen, 1958; Pichavant, 1981; Schmidt et al., 1997). Brines were prepared so that the total chloride concentration corresponded to the subcritical, "liquid-only" phase stability field in the NaCl-KCl-$H_2O$ system (determined by the data of Chou, 1987; Chou et al., 1992; Anderko and Pitzer, 1993a, b). The system NaCl-KCl-$H_2O$ was used to provide a first-order approximation of the colligative properties of our NaCl-KCl-HCl-$H_2O$ solution. Capsules were crimped, weighed, and sealed with a carbon electrode arc welder. During the closure weld, the capsules were chilled with dry ice to minimize vaporization of the volatile components.

Experiments were conducted in cold-seal pressure vessels. The vessels (René 41) were heated externally by way of alumina tube furnaces fitted with Kanthal windings. The furnaces were doubly wound, minimizing thermal gradients across the capsule, and with the hot end of the vessel inclined at 12° (relative to the horizontal) to minimize convection. Temperatures were measured with type K (Chromel-Alumel) external thermocouples positioned close to the midpoint of the capsule. External thermocouple readings were calibrated against readings from internal thermocouples under run conditions and found to be within ±2°C. The position of the internal thermocouple was varied to determine the gradient across the length of the capsule (±3°C). Run pressures were achieved by a pressure intensifier with water as the pressure medium and monitored with Bourdon-tube gauges (±2 MPa) that were calibrated against a factory-calibrated Heise gauge.

Experiments were quenched isobarically by removing the vessel from the furnace and placing it in a stream of compressed air while open to a large-reservoir pressure buffer set to 100 MPa. This method cools the vessel to <300°C in ~1 min. The vessel was then placed in a reservoir of water to complete the quench to room temperature. Total quench time is ~2 min. The capsules were removed from the vessels, cleaned, and weighed to check for any leakage during the experiments. Capsules exhibiting a weight loss ≥0.3 mg at any point of the experimental procedure were discarded. Table 3 lists the starting materials and duration of each experiment.

Run duration was varied and numerous replicate experiments were performed to determine if equilibrium had been obtained. This study

Table 2. Starting chemical composition of synthetic glass.

| Oxide | wt% (as oxide) |
|---|---|
| $Na_2O$ | 3.67 |
| $K_2O$ | 4.43 |
| CaO | 0.17 |
| $Fe_2O_3$ | 0.04 |
| $Al_2O_3$ | 11.09 |
| $SiO_2$ | 75.18 |
| $TiO_2$ | 0.03 |
| MnO | 0.01 |
| MgO | 0.10 |
| $P_2O_5$ | 0.03 |
| LOI[a] | 4.51 |
| Total | 99.26 |

[a] LOI = loss on ignition. Analysis performed by Activation Laboratories by XRF.

Table 3. Summary of experimental conditions (uncertainties for mass measurements are 0.1 mg).[a]

| Run | Chloride (wt%) | Starting KCl/NaCl | Starting KCl/HCl | Glass (mg) | Solution (mg) | Duration (h) |
|---|---|---|---|---|---|---|
| 1 | 42.5 ± 0.1 | 1.00 ± 0.01 | 104 ± 2 | 54.1 | 39.5 | 549.2 |
| 2 | 42.5 ± 0.1 | 1.00 ± 0.01 | 104 ± 2 | 41.4 | 39.5 | 186.2 |
| 3 | 42.5 ± 0.1 | 1.00 ± 0.01 | 104 ± 2 | 44.4 | 39.5 | 475.0 |
| 4 | 42.5 ± 0.1 | 1.00 ± 0.01 | 104 ± 2 | 68.4 | 39.5 | 359.8 |
| 5 | 42.5 ± 0.1 | 1.00 ± 0.01 | 104 ± 2 | 55.0 | 39.5 | 512.2 |
| 6 | 42.5 ± 0.1 | 1.00 ± 0.01 | 104 ± 2 | 35.2 | 39.5 | 742.8 |
| 7 | 42.5 ± 0.1 | 1.00 ± 0.01 | 104 ± 2 | 38.3 | 39.5 | 742.9 |
| 8 | 42.5 ± 0.1 | 1.00 ± 0.01 | 104 ± 2 | 50.0 | 39.5 | 453.2 |
| 9 | 42.5 ± 0.1 | 1.00 ± 0.01 | 104 ± 2 | 65.2 | 39.5 | 885.5 |
| 10 | 42.5 ± 0.1 | 1.00 ± 0.01 | 104 ± 2 | 48.8 | 39.5 | 885.0 |
| 11 | 42.5 ± 0.1 | 1.00 ± 0.01 | 750 ± 8 | 50.3 | 37.8 | 146.0 |
| 12 | 42.5 ± 0.1 | 1.00 ± 0.01 | 10.9 ± 0.1 | 53.8 | 39.7 | 334.9 |
| 13 | 42.5 ± 0.1 | 1.00 ± 0.01 | 10.9 ± 0.1 | 50.0 | 39.7 | 333.2 |
| 14 | 42.5 ± 0.1 | 1.00 ± 0.01 | 10.9 ± 0.1 | 43.4 | 39.7 | 232.0 |
| 15 | 42.5 ± 0.1 | 1.00 ± 0.01 | 5.30 ± 0.08 | 48.3 | 37.4 | 520.2 |
| 16 | 42.5 ± 0.1 | 1.00 ± 0.01 | 5.30 ± 0.08 | 49.4 | 37.4 | 503.5 |
| 17 | 42.5 ± 0.1 | 1.00 ± 0.01 | 5.30 ± 0.08 | 49.7 | 39.7 | 279.0 |
| 18 | 42.5 ± 0.1 | 1.00 ± 0.01 | 5.30 ± 0.08 | 53.4 | 39.7 | 278.5 |
| 19 | 42.5 ± 0.1 | 1.00 ± 0.01 | 5.30 ± 0.08 | 62.1 | 39.7 | 211.8 |
| 20 | 42.5 ± 0.1 | 1.00 ± 0.01 | 5.30 ± 0.08 | 56.2 | 39.7 | 307.5 |
| 21 | 42.5 ± 0.1 | 1.00 ± 0.01 | 5.30 ± 0.08 | 48.3 | 39.7 | 309.8 |
| 22 | 42.5 ± 0.1 | 1.00 ± 0.01 | 10.9 ± 0.1 | 60.6 | 39.7 | 326.7 |
| 23 | 42.5 ± 0.1 | 1.00 ± 0.01 | 130 ± 6 | 48.9 | 39.7 | 160.2 |
| 24 | 42.5 ± 0.1 | 1.00 ± 0.01 | 10.9 ± 0.1 | 58.4 | 79.5 | 244.0 |
| 25 | 42.5 ± 0.1 | 1.00 ± 0.01 | 10.9 ± 0.1 | 39.0 | 79.5 | 581.7 |
| 26 | 42.5 ± 0.1 | 1.00 ± 0.01 | 10.9 ± 0.1 | 68.1 | 79.5 | 575.2 |
| 27 | 42.5 ± 0.1 | 1.00 ± 0.01 | 10.9 ± 0.1 | 57.2 | 159.0 | 308.3 |
| 28 | 42.5 ± 0.1 | 1.00 ± 0.01 | 10.9 ± 0.1 | 80.7 | 79.5 | 383.0 |
| 29 | 42.5 ± 0.1 | 1.00 ± 0.01 | 10.9 ± 0.1 | 51.6 | 79.5 | 208.2 |
| 30 | 42.5 ± 0.1 | 1.00 ± 0.01 | 10.9 ± 0.1 | 49.5 | 79.5 | 287.3 |
| 31 | 42.5 ± 0.1 | 1.00 ± 0.01 | 5.17 ± 0.07 | 55.0 | 74.9 | 92.7 |
| 32 | 42.5 ± 0.1 | 1.00 ± 0.01 | 5.17 ± 0.07 | 41.6 | 74.9 | 669.2 |
| 33 | 42.5 ± 0.1 | 1.00 ± 0.01 | 5.17 ± 0.07 | 49.4 | 74.9 | 756.5 |
| 34 | 42.5 ± 0.1 | 0.500 ± 0.004 | 3.20 ± 0.04 | 67.0 | 67.5 | 140.0 |
| 35 | 42.5 ± 0.1 | 0.500 ± 0.004 | 3.20 ± 0.04 | 50.8 | 67.5 | 494.5 |
| 36 | 1.81 ± 0.03 | 1.00 ± 0.01 | 2.01 ± 0.01 | 47.9 | 40.0 | 504.0 |
| 37 | 1.03 ± 0.03 | — | — | 36.0 | 20.0 | 164.8 |
| 38 | 1.81 ± 0.03 | 1.00 ± 0.01 | 2.01 ± 0.01 | 48.0 | 100.0 | 188.7 |
| 39 | 1.81 ± 0.03 | 1.00 ± 0.01 | 2.01 ± 0.01 | 52.6 | 100.0 | 162.0 |

[a] All experiments were performed at 800°C and 100 ± 2 MPa. The KCl/NaCl and KCl/HCl values listed above are representative of the starting composition of the brine and are not equilibrium values. We varied the durations of the experiments to demonstrate equilibrium with respect to time (i.e., no change in alkali concentration and partitioning as a function of time).

used time invariance as a measure of the approach to equilibrium. Time invariance is a necessary, although not sufficient, condition of equilibrium and is evaluated by performing experiments of varying durations. Equilibrium is defined as no appreciable net change with time (in a closed system). Thus, with increasing time and at similar experimental conditions (temperature, pressure, etc.), the observed compositions of the glass and brine should cluster about some value (the mean) if equilibrium has been reached. Experiments in this study were varied in duration from 92.7 to 885.5 h and showed no time dependence over this range. These results are similar to those of Candela and Holland (1984) and Williams et al. (1995, 1997) where equilibrium between a melt and MVP was thought to have been attained within 4 d.

### 2.2. Analytical Procedures

Analyses of major elements (Si, Al, K, Na, Ca, Fe, Cl) in glass run products were accomplished with a JEOL 8900 electron microprobe (EPMA). Representative fragments of glass run products were mounted in plastic epoxy and polished with 220 SiC grit, 600 SiC grit, 3-$\mu$m diamond paste, and 0.03-$\mu$m alumina powder successively. Samples were prepared for analysis by coating them with approximately 300 Å of carbon by standard thermal evaporation techniques. EPMA analyses were performed at 15 kV and 5 nA with counting times ranging from 20 to 120 s (sum of peak and background). Each glass was analyzed at 10 points to evaluate homogeneity. X-ray intensities for each element were corrected with a primary and secondary standard (primary = Yellowstone rhyolite [NMNH 72854 VG568] and secondary = Tulancingo rhyolite [USGS RLS 132]). The compositions of the starting materials were compared with those of the run products to calculate the mass transfer of cations that may have occurred during the experiments.

Conservation of mass in a closed systems states that the number of moles of any element in the initial glass plus initial aqueous phase must be equivalent to the moles of that element in the final glass plus the final aqueous phase. Mass balance was used to calculate the final composition of the aqueous phase (fap) from the initial concentration of the glass (ig) and aqueous phase (iap) and final composition of the glass (fg). The concentration of sodium in the final aqueous phase was calculated by the relation

$$m_{Na}^{ig} + m_{Na}^{iap} = m_{Na}^{fg} + m_{Na}^{fap} \quad (1)$$

and

$$(g^{ig} \times C^{ig}_{Na}) + (g^{iap} \times C^{iap}_{Na}) = (g^{fg} \times C^{fg}_{Na}) + (g^{fap} \times C^{fap}_{Na}) \quad (2)$$

where $m^y_x$ is the number of moles of component x in phase y, $g^{iap}$ is the grams of initial aqueous phase ($g^{fap}$ is the grams of final aqueous phase), $g^{ig}$ is the grams of initial glass ($g^{fg}$ is the grams of final glass), $C^{ig}_{Na}$ is the concentration of sodium in the initial glass ($C^{fg}_{Na}$ indicates final glass) and $C^{iap}_{Na}$ is the concentration of sodium in the initial aqueous phase (fap indicates final aqueous phase). C is defined as mol/g and is calculated for the glass by

$$C^g_{Na}\left(\frac{\text{mole}}{\text{grams}}\right) = \left[\frac{\text{wt\% } Na_2O^g}{\text{Molecular Weight } Na_2O} \times 100 \times 2\right], \quad (3)$$

because wt% $Na_2O^g$ is equivalent to grams $Na_2O$/100 g glass, the ratio must be multiplied by 100 to convert to g/mol and multiplied by 2 to account for 2 mol of Na per 1 mol $Na_2O$. The mass of the glass and brine do not change during the experiment, so a simplified equations is

$$g^g \times (C^{ig}_{Na} - C^{fg}_{Na}) = g^b \times (C^{fap}_{Na} \times C^{iap}_{Na}) \quad (4)$$

where $g^g$ and $g^b$ are the grams of glass and brine, respectively. The concentration of sodium in the aqueous phase at equilibrium, $C^{fap}_{Na}$, is calculated through the following relation (an equivalent calculation is made for potassium)

$$C^{fap}_{Na} = C^{iap}_{Na} + \left[\frac{g^g}{g^b} \times (C^{ig}_{Na} - C^{fg}_{Na})\right]. \quad (5)$$

The calculation of HCl had to be conducted in a different manner because direct measurement of hydrogen in the glass was not possible. HCl concentrations can be calculated by

$$m^{fap}_{HCl} = m^{fap}_{Cl} - [m^{fap}_{NaCl} + m^{fap}_{KCl} + 2 \times (m^{fap}_{CaCl_2})]. \quad (6)$$

where $m^{fap}_{Cl}$, $m^{fap}_{NaCl}$, $m^{fap}_{KCl}$, and $m^{fap}_{CaCl_2}$ are moles of chloride, NaCl, KCl, and $CaCl_2$ in the aqueous phase, respectively. Although $CaCl_2$ was not present in the initial aqueous phase, some calcium was partitioned from the melt into the aqueous phase, most likely as the chloride complex $CaCl_2$.

## 3. RESULTS

### 3.1. Electron Microprobe Measurement of Glass Composition

The composition of the melt in each experiment was altered systematically as a result of interaction with the brine. The melt became enriched in some components and depleted in others (see Table 2 for starting compositions and Table 4 for equilibrium compositions of the melt). Figure 1 is a plot of the mole fraction of major components in the melt as a function of the HCl of a coexisting brine (all data displayed are for brine-only experiments). Some components (e.g., $SiO_2$ and $Al_2O_3$) were unaffected by increases in the concentration of HCl in a coexisting brine (i.e., slopes ~0.0). On the other hand, the concentration of chloride and potassium in the melt increased with increasing HCl in the brine, as illustrated by slopes of 0.07 and 0.08 (0.04 for $K_2O$), respectively; whereas sodium was removed partially from the melt (slope of −0.20 for $NaO_{0.5}$ and −0.10 for $Na_2O$).

At low HCl concentrations in the brine, the enrichment of potassium in the melt was greater in magnitude than the depletion of sodium and calcium, resulting in an enrichment of alkalis in the melt relative to aluminum. The ratio of potassium to sodium in the melt was close to unity at low HCl concentrations (~0.1 wt%), but rose to two at high concentrations of HCl (~0.4 wt%) in the brine. High concentrations of HCl in the brine preferentially removed sodium from the melt relative to aluminum and decreased the alkali:aluminum ratio of the melt.

Melt aluminosity can be described by the aluminum saturation index (ASI) as defined by Shand (1951). ASI values [molar: $Al_2O_3/(CaO + K_2O + Na_2O)] > 1.0$ indicate an excess of aluminum in the melt relative to alkalis. The composition of the starting glass has an ASI of 1.0, and Al/(Na + K) of 1.02; that is, the melts are near subaluminous. Melt aluminosity has been shown to be of major importance in controlling the composition of an exsolving MVP, with a highly aluminous melt producing a MVP with a high HCl concentration (Candela, 1990; Candela and Piccoli, 1995; Williams et al., 1997).

## 4. THERMODYNAMIC MODELING

### 4.1. Partition Coefficients

A Nernst-type partition coefficient ($D^{x/y}_i$) can be defined for the partitioning of an element i between phases x and y as

$$D^{x/y}_i = \frac{C^x_i}{C^y_i} \quad (7)$$

where $C^x_i$ and $C^y_i$ are the concentrations in wt% of element i in phases x and y, respectively. Concentrations of potassium and sodium in the melts were obtained through electron microprobe analyses of the glasses, and equilibrium brine compositions were calculated by mass balance constraints (as described in section 2.2). The partition coefficient for potassium between brine and melt, $D^{b/m}_K$, decreased slightly from 3.3 at $C^b_{HCl}$ = 0.03 wt% to 3.1 at $C^b_{HCl}$ = 3.5 wt%. With increasing $C^b_{HCl}$, from 0.03 to 3.5 wt%, $D_{Na}{}^{b/m}$ increased from 4.2 to 10.3. The variation in partition coefficients indicates that there was an exchange of potassium and sodium between the melt and brine and suggests that sodium components in the melt were less stable than potassium components as $C^b_{HCl}$ was increased. Although $D^{x/y}_i$ offers a simple method for estimating element exchange, it does not elucidate the processes of exchange nor the pertinent speciation. Equilibrium constants, which are presented in later sections, impart a much more robust method of evaluating element exchange.

### 4.2. Equilibrium Constants

There are a number of ways of treating the thermodynamics of multisite elements in solutions. Here, we choose to model homogeneous reactions among melt components.[1] When performing this type of analysis based entirely on analytical data, hypotheses for the existence of species by examining their consistency with the associated mass action laws (homogenous equilibria) that are used to describe the observed data. We will assume initially that all of the alkali elements are associated with the aluminate component of the melt as a first approximation. The exchange of alkali elements between the aluminate charge-balancing site in silicate melts and coexisting MVP can be explained by equilibria such as

[1] Components need not be species present in the system. They are simply algebraic representations of the chemical variability of a given phase or system.

Table 4. Analyses of major elements for glass run products (wt%).

| Run | $Na_2O$ | $K_2O$ | CaO | FeO | $Al_2O_3$ | $SiO_2$ | Cl | Total |
|---|---|---|---|---|---|---|---|---|
| 1 | 2.70 ± 0.19 | 6.15 ± 0.05 | 0.07 ± 0.02 | bd | 10.14 ± 0.12 | 74.85 ± 0.36 | 0.18 ± 0.01 | 94.09 |
| 2 | 2.66 ± 0.08 | 6.14 ± 0.15 | bd | bd | 10.52 ± 0.20 | 75.2 ± 0.6 | 0.18 ± 0.01 | 94.65 |
| 3 | 2.70 ± 0.09 | 6.45 ± 0.15 | 0.05 ± 0.01 | 0.17 ± 0.06 | 10.77 ± 0.22 | 76.22 ± 0.45 | 0.18 ± 0.01 | 96.54 |
| 4 | 2.76 ± 0.08 | 5.97 ± 0.06 | 0.03 ± 0.02 | 0.26 ± 0.04 | 10.75 ± 0.20 | 75.33 ± 0.35 | 0.16 ± 0.02 | 95.26 |
| 5 | 2.77 ± 0.14 | 6.47 ± 0.21 | 0.08 ± 0.04 | 0.07 ± 0.04 | 11.05 ± 0.28 | 74.1 ± 0.6 | 0.24 ± 0.02 | 94.80 |
| 6 | 2.69 ± 0.08 | 6.40 ± 0.10 | 0.04 ± 0.02 | 0.10 ± 0.05 | 11.15 ± 0.24 | 75.7 ± 0.6 | 0.22 ± 0.02 | 96.28 |
| 7 | 2.79 ± 0.12 | 6.42 ± 0.14 | bd | bd | 11.04 ± 0.25 | 75.00 ± 0.33 | 0.20 ± 0.01 | 95.45 |
| 8 | 2.71 ± 0.06 | 6.05 ± 0.06 | bd | 0.04 ± 0.02 | 10.88 ± 0.12 | 75.69 ± 0.33 | 0.16 ± 0.02 | 95.53 |
| 9 | 2.88 ± 0.19 | 6.17 ± 0.10 | bd | bd | 10.80 ± 0.15 | 75.26 ± 0.40 | 0.17 ± 0.01 | 95.28 |
| 10 | 2.46 ± 0.08 | 6.10 ± 0.06 | 0.04 ± 0.02 | 0.18 ± 0.06 | 10.75 ± 0.14 | 75.74 ± 0.17 | 0.18 ± 0.02 | 95.45 |
| 11 | 3.44 ± 0.31 | 4.94 ± 0.24 | 0.04 ± 0.02 | 0.08 ± 0.02 | 10.7 ± 0.8 | 77.1 ± 0.9 | 0.13 ± 0.01 | 96.46 |
| 12 | 2.30 ± 0.08 | 6.51 ± 0.25 | 0.02 ± 0.01 | 0.12 ± 0.02 | 10.35 ± 0.32 | 74.2 ± 0.8 | 0.23 ± 0.02 | 93.68 |
| 13 | 2.01 ± 0.18 | 6.63 ± 0.09 | 0.14 ± 0.04 | bd | 10.45 ± 0.21 | 73.01 ± 0.45 | 0.29 ± 0.04 | 92.53 |
| 14 | 1.97 ± 0.12 | 6.41 ± 0.24 | 0.13 ± 0.05 | 0.11 ± 0.04 | 10.18 ± 0.43 | 73.1 ± 0.8 | 0.21 ± 0.01 | 92.11 |
| 15 | 2.43 ± 0.22 | 6.51 ± 0.13 | 0.16 ± 0.05 | 0.07 ± 0.03 | 10.24 ± 0.11 | 72.51 ± 0.38 | 0.22 ± 0.02 | 92.14 |
| 16 | 2.05 ± 0.09 | 6.48 ± 0.32 | 0.04 ± 0.02 | 0.07 ± 0.03 | 10.10 ± 0.40 | 72.6 ± 1.0 | 0.27 ± 0.03 | 91.60 |
| 17 | 2.28 ± 0.26 | 6.32 ± 0.21 | 0.10 ± 0.02 | bd | 10.00 ± 0.45 | 73.6 ± 0.8 | 0.26 ± 0.05 | 92.58 |
| 18 | 2.37 ± 0.08 | 6.83 ± 0.09 | 0.08 ± 0.02 | 0.06 ± 0.03 | 10.88 ± 0.07 | 73.0 ± 0.7 | 0.26 ± 0.02 | 93.49 |
| 19 | 2.29 ± 0.16 | 6.66 ± 0.07 | bd | bd | 10.42 ± 0.26 | 72.2 ± 0.8 | 0.31 ± 0.08 | 91.92 |
| 20 | 2.16 ± 0.16 | 6.38 ± 0.13 | 0.04 ± 0.02 | 0.04 ± 0.02 | 10.67 ± 0.26 | 73.55 ± 0.48 | 0.24 ± 0.01 | 93.08 |
| 21 | 2.23 ± 0.22 | 6.52 ± 0.20 | bd | 0.10 ± 0.04 | 10.56 ± 0.35 | 73.1 ± 0.8 | 0.25 ± 0.03 | 92.79 |
| 22 | 2.06 ± 0.16 | 7.00 ± 0.11 | 0.13 ± 0.04 | bd | 10.63 ± 0.26 | 71.70 ± 0.38 | 0.23 ± 0.02 | 91.75 |
| 23 | 3.21 ± 0.16 | 4.17 ± 0.09 | 0.07 ± 0.03 | 0.11 ± 0.04 | 10.64 ± 0.33 | 74.4 ± 0.6 | 0.19 ± 0.01 | 92.78 |
| 24 | 2.29 ± 0.17 | 6.90 ± 0.09 | bd | bd | 10.54 ± 0.17 | 75.18 ± 0.16 | 0.26 ± 0.01 | 95.17 |
| 25 | 1.90 ± 0.21 | 6.90 ± 0.09 | bd | 0.02 ± 0.01 | 11.18 ± 0.18 | 74.46 ± 0.40 | 0.21 ± 0.01 | 94.67 |
| 26 | 1.81 ± 0.17 | 6.79 ± 0.12 | 0.07 ± 0.02 | 0.04 ± 0.02 | 10.67 ± 0.15 | 74.36 ± 0.35 | 0.18 ± 0.02 | 93.92 |
| 27 | 1.82 ± 0.22 | 6.92 ± 0.15 | 0.01 ± 0.01 | 0.05 ± 0.02 | 11.45 ± 0.45 | 73.7 ± 0.6 | 0.26 ± 0.02 | 94.25 |
| 28 | 1.96 ± 0.22 | 6.64 ± 0.13 | 0.03 ± 0.02 | 0.03 ± 0.02 | 10.56 ± 0.17 | 75.38 ± 0.45 | 0.18 ± 0.01 | 94.78 |
| 29 | 2.13 ± 0.28 | 6.70 ± 0.12 | 0.05 ± 0.02 | 0.05 ± 0.02 | 10.64 ± 0.22 | 75.68 ± 0.37 | 0.20 ± 0.01 | 95.45 |
| 30 | 1.89 ± 0.13 | 6.92 ± 0.15 | 0.04 ± 0.02 | 0.06 ± 0.03 | 10.52 ± 0.35 | 74.79 ± 0.45 | 0.24 ± 0.02 | 94.46 |
| 31 | 1.97 ± 0.06 | 6.78 ± 0.08 | 0.01 ± 0.01 | 0.06 ± 0.03 | 10.57 ± 0.24 | 75.1 ± 0.5 | 0.25 ± 0.02 | 94.78 |
| 32 | 1.99 ± 0.16 | 6.92 ± 0.18 | 0.04 ± 0.02 | 0.04 ± 0.02 | 10.71 ± 0.21 | 75.64 ± 0.49 | 0.20 ± 0.01 | 95.54 |
| 33 | 2.08 ± 0.13 | 6.40 ± 0.25 | bd | bd | 10.35 ± 0.33 | 76.0 ± 0.9 | 0.29 ± 0.02 | 95.16 |
| 34 | 3.44 ± 0.20 | 5.36 ± 0.12 | 0.05 ± 0.02 | 0.03 ± 0.01 | 10.75 ± 0.23 | 76.10 ± 0.44 | 0.28 ± 0.06 | 96.01 |
| 35 | 2.96 ± 0.24 | 5.34 ± 0.15 | bd | bd | 11.10 ± 0.14 | 75.47 ± 0.38 | 0.24 ± 0.01 | 95.11 |
| 36 | 3.74 ± 0.26 | 4.62 ± 0.14 | bd | 0.09 ± 0.03 | 10.54 ± 0.38 | 71.5 ± 0.7 | 0.24 ± 0.02 | 90.72 |
| 37 | 3.55 ± 0.22 | 4.33 ± 0.06 | bd | bd | 10.75 ± 0.14 | 74.91 ± 0.25 | 0.06 ± 0.01 | 93.60 |
| 38 | 3.54 ± 0.25 | 5.16 ± 0.08 | bd | bd | 10.93 ± 0.27 | 73.73 ± 0.38 | 0.21 ± 0.02 | 93.57 |
| 39 | 3.41 ± 0.28 | 4.83 ± 0.12 | bd | bd | 10.32 ± 0.28 | 73.8 ± 0.6 | 0.15 ± 0.02 | 92.54 |

Each glass was analyzed in 10 separate areas of the sample to evaluate glass homogeneity. X-ray intensities for each element were corrected using two standards (Yellowstone rhyolite and Tulancingo rhyolite). Uncertainties are presented as the standard deviation from the mean ($1\sigma$) for the 10 measurements of each glass. bd = value below detection.

$$NaCl^b + KAlO_2^m = NaAlO_2^m + KCl^b \quad (8)$$

for the exchange of sodium and potassium between melt and brine. Here, the sodium and potassium in the silicate melt play a charge-balancing role and are represented by $NaAlO_2$ and $KAlO_2$, respectively. An equilibrium constant, $K_{ex}$ (K, Na), for the exchange of potassium and sodium between aluminate and chloride components, Eqn. 8, can be written as

$$K_{ex}\,(K, Na) = \frac{a^m_{NaAlO_2} \times a^b_{KCl}}{a^b_{NaCl} \times a^m_{KAlO_2}} \quad (9)$$

where $a^m_{NaAlO_2}$, $a^m_{KAlO_2}$, $a^b_{NaCl}$, and $a^b_{KCl}$ are the activities of $NaAlO_2$ in the melt, $KAlO_2$ in the melt, NaCl in the brine, and KCl in the brine, respectively. Because we are unable to determine the activities of the components directly, we have used concentrations to calculate an apparent equilibrium constant for Eqn. 8, denoted as $K'_{ex}$ (K, Na) and represented by

$$K'_{ex}\,(K, Na) = \frac{C^m_{NaAlO_2} \times C^b_{KCl}}{C^b_{NaCl} \times C^m_{KAlO_2}}. \quad (10)$$

We evaluated the aluminate–chloride component model by comparing the apparent equilibrium constant, $K'_{ex}$ (K, Na), to the empirical (analytical) $K'_{meas}$ (K, Na). $K'_{meas}$ (K, Na) accounts for all sodium and potassium in the melt, is defined by

$$K'_{meas}\,(K, Na) = \frac{C^m_{Na} \times C^b_{KCl}}{C^b_{NaCl} \times C^m_{K}} = \frac{D^{b/m}_{K}}{D^{b/m}_{Na}} \quad (11)$$

and does not distinguish among the alkali components or species present in the melt.

Varying the starting KCl/NaCl of the brine, at a constant total chloride, had no effect on the $K'_{meas}$ (K, Na). Therefore, our data support the aluminate–chloride model outlined above with respect to variations in KCl/NaCl.

The assumption that $K'_{meas}$ (K, Na) was an accurate representation of $K'_{ex}$ (K, Na) was further tested by varying the HCl concentration in the brine. HCl is not included in the equilibrium, Eqn. 8, so $K'_{meas}$ (K, Na) should not be affected as a result of mass actions by variations in $C^b_{HCl}$ and should remain an accurate representation of $K'_{ex}$ (K, Na). However,

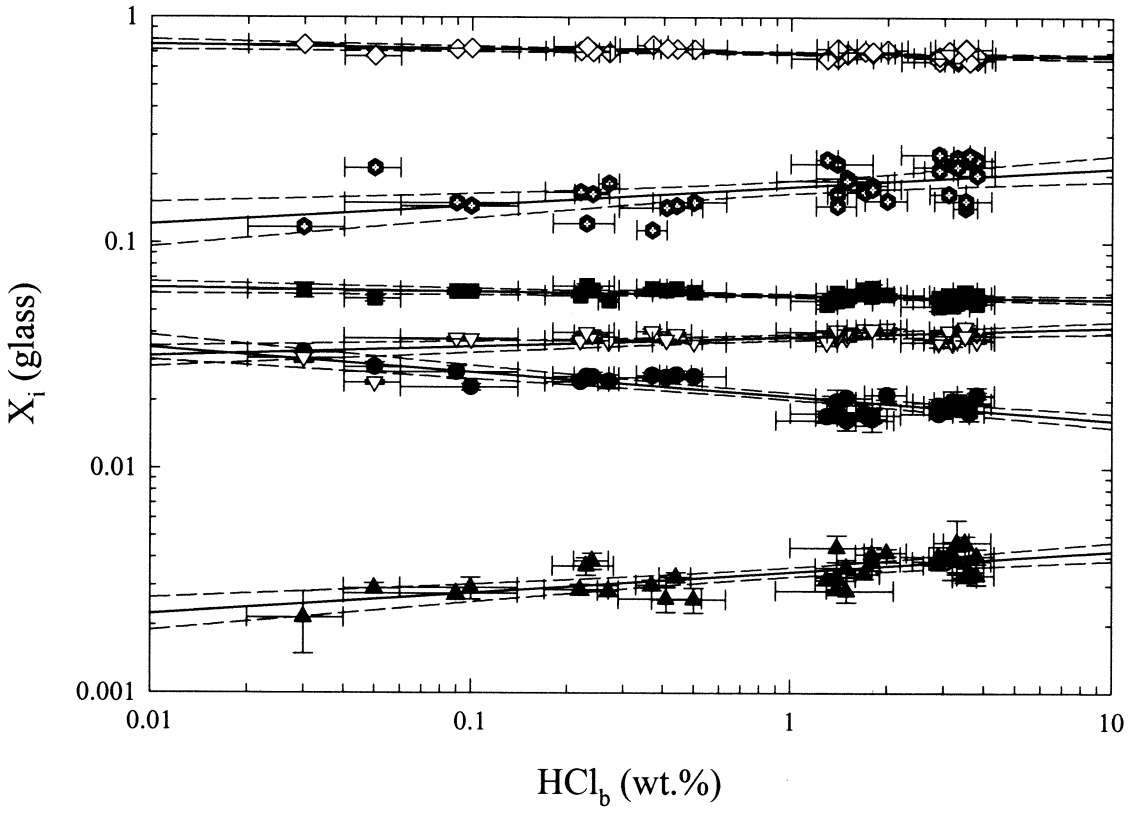


Fig. 1. Mole fraction ($X_i$) of the major components of the melt as a function of the HCl concentration of a coexisting brine. $SiO_2$, $H_2O$, $Al_2O_3$, $K_2O$, $Na_2O$, and Cl are represented by open diamonds, open hexagons, squares, inverted open triangles, circles, and triangles, respectively. The solid line through data for each element is a line of linear regression, and the dashed line is the 95% confidence interval. Error bars on each data point are due to analytical and experimental uncertainty and are $1\sigma$.

[$K'_{meas}$ (K, Na)] was found to vary inversely with $C^b_{HCl}$ (Fig. 2, Table 5), suggesting that $K'_{ex}$ (K, Na) does not explain fully the exchange of alkali elements between the melt and brine. This suggests that alkali element exchange cannot be described simply as an aluminate–chloride exchange. The probability of a major nonchloride component in the brine is low, so the reasonable assumption is that the alkali elements in the melt are not in charge balance roles only.

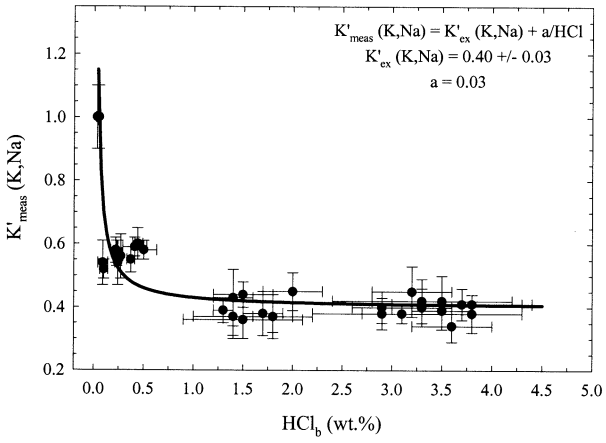


Fig. 2. $K'_{meas}$ (K, Na) values for brine–melt exchange of sodium and potassium as a function of the HCl concentration of a coexisting brine. The black line is the regressed line through the points based on the first-order polynomial. $K'_{ex}$ (K, Na) represent the apparent equilibrium constant for the exchange of sodium and potassium between aluminate and chloride components (0.40 ± 0.03; $1\sigma$), whereas a = 0.03 and is defined as a best-fit parameter.

Nuclear magnetic resonance (NMR) studies of silicate glasses conducted by Kohn et al. (1989, 1992, 1998) show that a portion of sodium present in water-saturated silicate melts is not present in a charge balancing role (defined here as the aluminate component), and is most likely complexed as NaOH. A recent study by Schmidt et al. (2001) in the orthoclase-albite-quartz-$H_2O$ system found that although the NMR data for the glasses could not exclude the presence of small amounts of Si-OH and Al-OH groups in the glasses, the total water content of the glasses correlated well with the observed $^{23}$Na isotropic shift. They concluded that their data are in general agreement with the water dissolution model proposed by Kohn et al. (1989), but that other mechanisms of water solubility may also be operative in subordinate roles. Therefore, it has been hypothesized (Kohn et al., 1989) that the NaOH component in water-saturated melts is controlled by the equilibrium

$$NaAlO_2^m + H_2O^{sys} = NaOH^m + HAlO_2^m, \qquad (12)$$

which is an expression of the exchange of protons for charge

Table 5. $K'_{meas}$ (K, Na) values for brine-melt exchange of sodium and potassium as a function of the HCl concentration of a coexisting brine. Uncertainties are calculated from the EPMA analyses and are $1\sigma$.

| Run | HCl (wt%) | $K'_{meas}$ (K, Na) |
|---|---|---|
| 1 | $2.7(\pm0.2) \times 10^{-1}$ | 0.56 ± 0.07 |
| 2 | $2.2(\pm0.5) \times 10^{-1}$ | 0.58 ± 0.04 |
| 3 | $3.7(\pm0.4) \times 10^{-1}$ | 0.55 ± 0.04 |
| 4 | $5.0(\pm1.3) \times 10^{-1}$ | 0.58 ± 0.03 |
| 5 | $2.4(\pm0.3) \times 10^{-1}$ | 0.54 ± 0.07 |
| 6 | $2.3(\pm0.5) \times 10^{-1}$ | 0.57 ± 0.04 |
| 7 | $4.4(\pm0.5) \times 10^{-1}$ | 0.60 ± 0.05 |
| 8 | $4.1(\pm1.2) \times 10^{-1}$ | 0.59 ± 0.03 |
| 9 | $0.9(\pm0.5) \times 10^{-1}$ | 0.54 ± 0.07 |
| 10 | $1.0(\pm0.4) \times 10^{-1}$ | 0.52 ± 0.03 |
| 11 | $0.3(\pm0.1) \times 10^{-1}$ | 1.0 ± 0.1 |
| 12 | 1.5(±0.3) | 0.44 ± 0.04 |
| 13 | 1.4(±0.4) | 0.37 ± 0.06 |
| 14 | 1.3(±0.1) | 0.39 ± 0.04 |
| 15 | 3.8(±0.5) | 0.38 ± 0.06 |
| 16 | 2.9(±0.7) | 0.38 ± 0.05 |
| 17 | 3.2(±0.4) | 0.45 ± 0.08 |
| 18 | 3.8(±0.5) | 0.41 ± 0.03 |
| 19 | 3.3(±0.3) | 0.40 ± 0.05 |
| 20 | 2.9(±0.3) | 0.40 ± 0.05 |
| 21 | 3.3(±0.9) | 0.42 ± 0.07 |
| 22 | 3.6(±0.3) | 0.34 ± 0.05 |
| 23 | $0.5(\pm0.1) \times 10^{-1}$ | 1.0 ± 0.1 |
| 24 | 2.0(±0.3) | 0.45 ± 0.06 |
| 25 | 1.7(±0.2) | 0.38 ± 0.07 |
| 26 | 1.5(±0.6) | 0.36 ± 0.06 |
| 27 | 1.8(±0.2) | 0.37 ± 0.07 |
| 28 | 1.4(±0.1) | 0.37 ± 0.07 |
| 29 | 1.4(±0.2) | 0.43 ± 0.09 |
| 30 | 1.8(±0.4) | 0.37 ± 0.05 |
| 31 | 3.1(±0.4) | 0.38 ± 0.03 |
| 32 | 3.5(±0.3) | 0.39 ± 0.06 |
| 33 | 3.5(±0.7) | 0.42 ± 0.08 |
| 34 | 3.7(±0.7) | 0.41 ± 0.05 |
| 35 | 3.3(±0.3) | 0.40 ± 0.06 |

balancing cations. A study by Mysen and Acton (1999) identified the presence of KOH in hydrated melts in the $K_2O$-$Al_2O_3$-$SiO_2$-$H_2O$ system through the use of Raman spectroscopy. This would imply that an equilibrium similar to Eqn. 12 would apply to potassium as well. However, on the basis of the increase in $D_{Na}^{b/m}$ with increasing $C_{HCl}^{b}$, together with the relative invariance of $D_{K}^{b/m}$ (which combined, result in a decrease in $K'_{meas}$ (K, Na)), we will initially model potassium as an aluminate component only.

In the limit where a large proportion of the potassium in the silicate melt can be accounted for as $KAlO_2$, whereas sodium is present dominantly as NaOH and $NaAlO_2$, an apparent equilibrium constant written to account for the sodium and potassium components is

$$K'_{meas}\,(K, Na) = \frac{(C^{m}_{NaAlO_2} + C^{m}_{NaOH}) \times C^{b}_{KCl}}{C^{b}_{NaCl} \times C^{m}_{KAlO_2}} = \frac{C^{m}_{NaAlO_2} \times C^{b}_{KCl}}{C^{b}_{NaCl} \times C^{m}_{KAlO_2}} + \frac{C^{m}_{NaOH} \times C^{b}_{KCl}}{C^{b}_{NaCl} \times C^{m}_{KAlO_2}} \quad (13)$$

or, more appropriately, because $K'_{ex}$ (K, Na) can be defined for the exchange of potassium and sodium between melt (aluminate components) and brine (chloride components)

$$K'_{meas}\,(K, Na) = K'_{ex}\,(K, Na) + \frac{C^{m}_{NaOH} \times C^{b}_{KCl}}{C^{b}_{NaCl} \times C^{m}_{KAlO_2}}. \quad (14)$$

The introduction of the NaOH component demands an additional homogeneous equilibrium, which can be written as a simple acid-base type equilibrium

$$HCl^{b} + NaOH^{m} = NaCl^{b} + H_2O^{sys} \quad (15)$$

with an apparent equilibrium constant defined as

$$K'\,(NaOH) = \frac{C^{b}_{NaCl} \times f^{sys}_{H_2O}}{C^{b}_{HCl} \times C^{m}_{NaOH}}. \quad (16)$$

Rearranging Eqn. 16 and solving for $C^{m}_{NaOH}$ yields

$$C^{m}_{NaOH} = \frac{C^{b}_{NaCl} \times f^{sys}_{H_2O}}{C^{b}_{HCl} \times K'\,(NaOH)}. \quad (17)$$

Substituting the relationship between $C^{m}_{NaOH}$ and Eqn. 17 into Eqn. 14 yields

$$K'_{meas}\,(K, Na) = K'_{ex}\,(K, Na) + \frac{f^{sys}_{H_2O} \times C^{b}_{KCl}}{K'\,(NaOH) \times C^{m}_{KAlO_2} \times C^{b}_{HCl}}, \quad (18)$$

which can be manipulated to form a mathematical model that may follow the trend of the data. The best-fit parameter, a, is defined as

$$a = \frac{f^{sys}_{H_2O} \times C^{b}_{KCl}}{K'\,(NaOH) \times C^{m}_{KAlO_2}}. \quad (19)$$

A relationship between $K'_{meas}$ (K, Na) and $K'_{ex}$ (K, Na) can be established as a function of $C^{b}_{HCl}$ through an inverse first order polynomial of the form

$$K'_{meas}\,(K, Na) = K'_{ex}\,(K, Na) + \frac{a}{C^{b}_{HCl}} \quad (20)$$

where $K'_{meas}$ (K, Na) is the empirical apparent equilibrium constant, $K'_{ex}$ (K, Na) is the apparent exchange equilibrium constant (equal to 0.40 ± 0.03; $1\sigma$), and a is a constant = 0.03 (Fig. 2). $K'_{ex}$ (K, Na) accounts for the exchange of sodium and potassium between chloride components in the brine and aluminate components in the melt (Fig. 2), and is the representation of the exchange equilibrium (Eqn. 8). An additional check on $K'_{ex}$ (K, Na) completed by taking the mean value of $K'_{meas}$ (K, Na) for all experiments with >1 wt% HCl, where the NaOH component of the melt is thought to be minimized, agrees well with the calculated best fit value for $K'_{ex}$ (K, Na).

Rearranging Eqn. 19 yields an equilibrium constant for Eqn. 16, which is given by

$$K'\,(NaOH) = \frac{f^{sys}_{H_2O} \times C^{b}_{KCl}}{(0.03) \times C^{m}_{KAlO_2}} = \frac{C^{b}_{NaCl} \times f^{sys}_{H_2O}}{C^{b}_{HCl} \times C^{m}_{NaOH}} \quad (21)$$

and yields

$$\frac{C^{b}_{NaCl}}{C^{m}_{NaOH}} = \frac{C^{b}_{HCl} \times C^{b}_{KCl}}{(0.03) \times C^{m}_{KAlO_2}}. \quad (22)$$

which allows a ratio for sodium present as chloride in the brine relative to hydroxide components in the melt to be calculated (Fig. 3). Note that increasing $C^{b}_{HCl}$ will drive the $NaOH^{m}$-

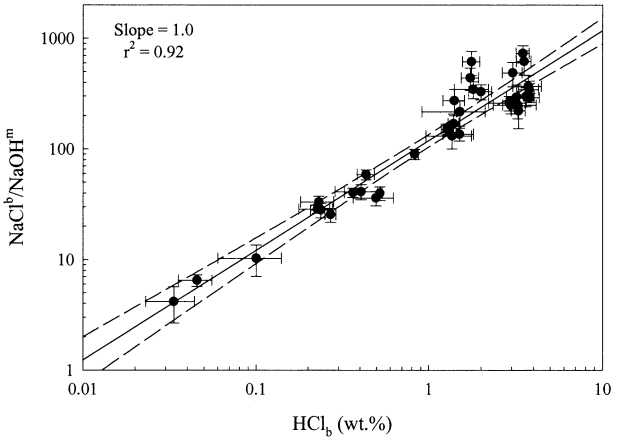


Fig. 3. Calculated values of $NaCl^b/NaOH^m$ reveal that the value increases as the HCl concentration of the coexisting brine increases. A linear line (solid line) regressed through the data has a slope = 1.0. The dashed lines represent the 95% confidence interval; $r^2 = 0.92$.

$NaCl^b$ equilibrium (Eqn. 15) to the right along with increasing $NaCl^b/NaOH^m$ in the system.

Note also that

$$\frac{C^m_{NaOH}}{C^m_{\Sigma Na}} = \frac{C^m_{NaOH}}{C^b_{NaCl}} \times \frac{C^b_{NaCl}}{C^m_{\Sigma Na}} = \frac{C^m_{NaOH}}{C^b_{NaCl}} \times D^{b/m}_{Na}. \qquad (23)$$

That is, the proportion of NaOH relative to total sodium in the melt decreases with increasing $C^b_{HCl}$, as per Eqn. 15 (Fig. 4). Again, this is analogous to a simple acid/base reaction where an acid is neutralized by a base producing water and salt. In this case, the NaOH component in the melt is neutralized by HCl from the brine to produce NaCl and $H_2O$. The model developed here adequately describes the data presented in this study. Excluding the KOH component, observed by Mysen and Acton (1999) in a system where potassium was the only alkali element, from the model has not affected adversely the fit of the

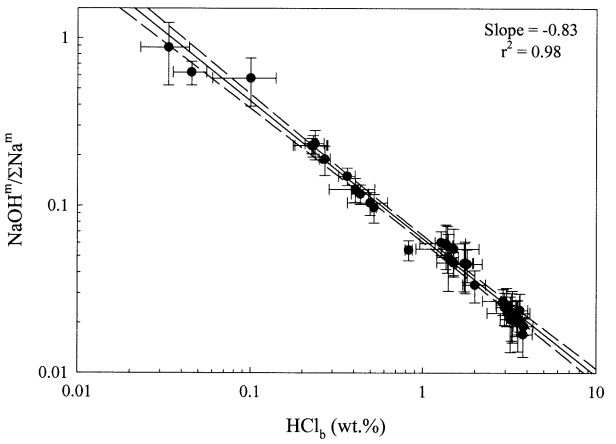


Fig. 4. Calculated values of NaOH/ΣNa in the melt indicates that NaOH in the melt became depleted as the HCl concentration of the coexisting brine increased. The solid line is a linear regression through the data (slope = −0.83); the dashed line is the 95% confidence interval ($r^2 = 0.98$).

model to the data. However, the correlation does not indicate that the KOH species does not exist in the melt, rather is simply suggests that KOH does not play a significant role in the "neutralization" of the HCl component of a magmatic volatile phase at the conditions of this study. If the melt in this study had a significant component of KOH, then the concentration of potassium in the melt could not be wholly accounted for by potassium aluminate. This would serve to increase both the $K'_{meas}$ (K, Na) and $K'_{ex}$ (K, Na) values as a result of a decrease in the potassium aluminate value.

## 5. DISCUSSION

### 5.1. Element Exchange between a Brine and Silicate Melt as a Function of HCl

The mechanism of hydration in silicate melts has been of great interest and thus the subject of many studies (Stolper, 1982; Mysen and Virgo, 1986; Kohn et al., 1989, 1992; Holtz et al., 1992, 1995; Nowak and Behrens, 1995; Shen and Keppler, 1995; Mysen and Wheeler, 2000; Schmidt et al., 2001). Many studies (Holtz et al., 1992, 1995; Yamashita, 1999) have concluded that the solubility of water in a haplogranitic melt is 4 to 5 wt% at 800°C and 100 MPa. Stolper (1982) suggested, on the basis of studies of quenched glasses, that this much total water dissolved in the melt would correspond to ~2 wt% as hydroxyl and molecular water each. Shen and Keppler (1995) used near-infrared spectra taken of quenched glasses and melts in situ and related that the $H_2O/OH^-$ value of a quenched glass/melt was influenced by temperature, so much so that quenched glasses did not give the same $H_2O/OH^-$ values as melts in situ. Nowak and Behrens (1995) completed a study at 150 MPa and found that the proportion of hydroxyl to molecular water was a function of temperature, with molecular water comprising only ~1 wt% of the 4.14 ± 0.07 wt% total water in the melt at 800°C. The glasses in this study suggest the solubility of total water in the melt was 4 to 5 wt%, so following the work of Nowak and Behrens (1995), the melt in this study should contain ~3 wt% water as a hydroxyl component (~0.18 mol). There is little evidence for significant Si-OH groups in alkali aluminosilicate melts (Mysen and Virgo, 1986; Kohn et al., 1992; Schmidt et al., 2001); whereas the association of aluminum with OH groups in addition to the alkali-OH groups may also be a significant mechanism of hydration in silicate melts (Mysen and Wheeler, 2000). Although the Al-OH groups are important in many areas related to melt structure, these groups have little affect on our thermodynamic model because they are not involved in the chosen equilibria. Ultimately, these studies support the model derived here because they underlie the importance of hydroxyl groups in silicate melts and, further, indicate that a substantial alkali element-OH component is present.

This extensive work on melt structure and speciation allows us to formulate hypotheses involving melt-MVP interactions that can explain our results. Our data suggest the following: (1) melt hydration increased the activity of NaOH and $HAlO_2$ components in the melt; (2) HCl in the brine reacted with the sodium hydroxide component of the melt to produce $H_2O$; and (3) the NaOH component of the melt was more likely to exercise control over MVP acidity than the KOH component of

the melt. The majority of sodium chloride produced by the reaction involving the NaOH and HCl components fluxed into the brine, as evidenced by the increase in the partition coefficient for sodium between brine and melt. A similar equilibrium may exist for the KOH component of the melt, but the data are consistent with the NaOH component of the melt playing a much more significant role in interactions with a highly acidic volatile phase. Our results for sodium are consistent with the results of Kohn et al. (1989, 1994) and Schmidt et al. (2001), who suggested that sodium is partitioned between aluminate and hydroxide components in hydrated melts. A study by Mysen and Acton (1999) identified the presence of KOH in hydrated melts in the $K_2O$-$Al_2O_3$-$SiO_2$-$H_2O$ system through the use of Raman spectroscopy. Unfortunately, no work to date has focused on quantitative determination of KOH or NaOH in silicate melts.

Stolper (1982) studied the solubility and speciation of water in silicate melts and modeled the results by a quasichemical formulation given by

$$H_2O^m_{molecular} + O^m = 2\ OH^m \quad (24)$$

where $H_2O^m_{molecular}$ is molecular $H_2O$ in the melt, $O^m$ is bridging oxygen in the melt (i.e., oxygen that bridges two adjoining tetrahedral, network-forming cations), and $OH^m$ represents hydroxyl attached to a silicate polymer (includes both aluminate and hydroxyl components). The corresponding equilibrium constant is

$$K'\ (H_2O, OH) = \frac{(a^m_{OH})^2}{a^m_{H_2O_{molecular}} \times a^m_O} \quad (25)$$

where $a_{H_2}O^m_{molecular}$, $a^m_O$, and $a^m_{OH}$ refer, respectively, to the activities of molecular water, bridging oxygen, and hydroxyl groups in the melt. Allowing activities to be given by mole fractions yields K' ($H_2O$, OH) ~0.1 to 0.3 for Eqn. 25. In this quasichemical formulation, the hydroxyl groups from both NaOH and $HAlO_2$ components are represented by $a^m_{OH}$ in the equilibrium constant. The equilibrium constant dictates that as $a^m_{OH}$ decreases, the product $a^m_O \cdot a^m_{H_2O\ molecular}$ must decrease. The data suggest that the NaOH portion of $a^m_{OH}$ decreases through reaction with HCl, but the $HAlO_2$ portion of $a^m_{OH}$ does not. The absolute decrease in $a^m_{OH}$ is therefore small as the effect of neutralizing the NaOH component of the "total hydroxyl" is masked by the more abundant $HAlO_2$ component. By use of the equilibrium constant from Stolper (1982), the mole fraction of OH ($X^m_{OH}$) was calculated, and assuming that all of the NaOH in the melt reacts to form NaCl and $H_2O$, the decrease in $X^m_{OH}$ (assuming that $\gamma^m_{OH}$ is unity, and thus $a^m_{OH} = X^m_{OH}$) was calculated as ~7% relative. Therefore, although there was a change in the $NaOH^m/\Sigma Na^m$ on the order of two orders of magnitude, the resulting change in the OH component of the melt was small.

### 5.2. Comparison of Brine–Melt to Vapor or Supercritical Fluid–Melt Systems

Many workers have studied the exchange of elements between a MVP and silicate melt (Gammon et al., 1969; Holland, 1972; Shinohara, 1987; Williams et al., 1997; Schäfer et al., 1999; Student and Bodnar, 1999), although only a few of these studies monitored, much less controlled, the acidity of the volatile phase. The studies by Schäfer et al. (1999) and Student and Bodnar (1999) are examples of experimental studies that determined the distribution of alkali elements between low-salinity volatile phases and melts but did not report solution acidity. Schäfer et al. (1999) determined the partitioning of elements between a chloride-bearing aqueous phase and silicate melt via laser ablation inductively coupled plasma mass spectrometry analyses of the quenched glass and fluid inclusions contained within. They determined $K'_{meas}$ (K, Na) values of $0.49 \pm 0.12$ and $0.47 \pm 0.07$ for two experiments at 850°C and 200 MPa in the haplogranite-supercritical chloride-bearing fluid system. The study of Student and Bodnar (1999) produced coeval silicate melt and aqueous fluid inclusions at 800°C and 200 MPa in a quartz-saturated portion of the haplogranite-supercritical chloride-bearing fluid system. They reported a $K'_{meas}$ (K, Na) value of 0.40. These values are broadly consistent with the results reported in this study, but the absence of data on HCl in the aqueous phase or even the quench pH of the solution does not allow for a more detailed comparison to this study.

The pioneering work in this field was by Gammon et al. (1969) and Holland (1972), who measured the exchange of potassium and sodium between a MVP and silicate melt at temperatures ranging from 770 to 880°C and total pressures of 140 to 240 MPa. Unlike the present study, Gammon et al. (1969) performed experiments in the supercritical fluid field, with salinities varied from 1.9 to 34 wt% NaCl (equivalent). Measurements of pH of the quenched aqueous solutions revealed values typically between 1.4 and 2.2. These quench pH values indicate HCl was generated by the interaction of the supercritical fluid with the melt during the course of the experiment. The concentration of HCl in the supercritical fluid, as based on quench pH measurements in the quenched solutions, was $0.07 \pm 0.03$ wt%. Data were presented as $K'_{meas}$ (K, Na), which was found to be $0.74 \pm 0.03$ and independent of temperature and pressure over the range studied.

Shinohara (1987) conducted experiments with a supercritical fluid-silicate melt assemblage at a temperature of 810°C and a range of pressures (220 to 670 MPa) and compositions. Shinohara (1987) advanced the experiments performed by Gammon et al. (1969) and Holland (1972) by adding HCl to the starting aqueous fluids. Experiments performed at 220 MPa and 810°C exhibited a $K'_{meas}$ (K, Na) $= 0.60 \pm 0.11$. Shinohara found a systematic positive variation in $K'_{meas}$ (K, Na) as a function of the product of the concentration of chloride in the aqueous phase ($C^{scf}_{Cl}$) and the water/glass ratio of the experiment and assumed it was a consequence of an ion exchange reaction that occurred upon quench. Shinohara applied a correction to $K'_{meas}$ (K, Na) that was based on this observation and reported a $K'_{meas}$ (K, Na) of $0.75 \pm 0.05$ for all experiments with $C^{scf}_{HCl}$ ranging from $5 \times 10^{-3}$ to 0.5 wt%. Increasing $C^{scf}_{Cl}$ will not affect the ratio of sodium to potassium or hydrogen, but will increase the absolute concentrations of all chloride components in the melt. Additionally, low-HCl experiments will be buffered against large changes in HCl concentrations at high water/glass ratios, so we suggest that the variation in $K'_{meas}$ (K, Na) observed by Shinohara could be a result of variations in $C^{scf}_{HCl}$ and its effects on the potassium–sodium exchange.

In the experiments of Williams et al. (1997), the exchange of

Table 6. Listing of $K'_{meas}$ (K, Na) and $C^{v}_{HCl}$ values for vapor-silicate melt experiments. W16 represents experiment number 16 of Williams et al. (1997).

| Sample identification | $K'_{meas}$ (K, Na) | $C^{v}_{HCl}$ (wt%) |
|---|---|---|
| W16 | 0.83 | 0.22 |
| W17 | 0.78 | 0.11 |
| W18 | 0.79 | $5.5 \times 10^{-2}$ |
| W33 | 0.84 | $2.2 \times 10^{-2}$ |
| Average | 0.81 | — |
| SD ($2\sigma$) | 0.03 | — |

hydrogen relative to potassium and sodium, $K'_{meas}$ (H, Na) and $K'_{meas}$ (H, K) was determined for each experiment. Although they did not calculate $K'_{meas}$ (K, Na) from their data, values are calculated here for each experiment in the vapor–silicate melt system (Table 6). Experiments conducted in the Williams et al. (1997) study in the vapor–silicate melt system (n = 4) exhibited an average $K'_{meas}$ (K, Na) = 0.81 ± 0.02 at $C^{v}_{HCl}$ values ranging from $2.2 \times 10^{-2}$ to 0.22 wt%. There is scatter in the vapor-only silicate melt data and no relationship between HCl and $K'_{meas}$ (K, Na) could be discerned, but this may be the result of the low number of experiments conducted. Therefore, exploratory experiments (n = 4) were conducted, as part of the current study, with a 3 wt% NaCl (equivalent) aqueous solution for a vapor–silicate melt phase assemblage. HCl concentrations in the vapor ranged from 0.10 to 0.21 wt% as calculated by mass balance. The measured $K'_{meas}$ (K, Na) values are similar to $K'_{meas}$ (K, Na) values at equivalent $C_{HCl}$ in the brine–silicate melt assemblage (Table 7). Also, these values compare favorably to those determined by Gammon et al. (1969), Holland (1972), Shinohara (1987), and Williams et al. (1997). These data are for either supercritical fluid or vapor experiments and are compared with the results of both the brine–silicate melt and vapor–silicate melt values determined in this study (Fig. 5). There is excellent agreement between the aforementioned studies and the model presented herein. It appears that the relationship derived from the brine–silicate melt exchange equilibrium is of general applicability.

## 6. IMPLICATIONS

The knowledge of the thermodynamics of silicate melts over a range of pressure, temperature, and composition provides a basis for the characterization of important physical and chemical properties needed to describe igneous process that may affect magmatic–hydrothermal processes. The results from this study suggest that a melt with low model sodium hydroxide concentration relative to total sodium, and hence low-model sodium hydroxide relative to model sodium aluminate, will produce an MVP with a high $C^{MVP}_{HCl}$. The main control on the model $NaOH^m/\Sigma Na^m$ is the fugacity of $H_2O$ in the system, $f^{sys}_{H_2O}$, with increasing $f^{sys}_{H_2O}$ increasing $NaOH^m/\Sigma Na^m$. Although increases in $f^{sys}_{H_2O}$ increase the $NaOH^m/\Sigma Na^m$ and would decrease the $C^{MVP}_{HCl}$, the HCl/NaCl of an exsolving MVP will increase because HCl/NaCl in the brine is related to $NaOH^m/\Sigma Na^m$ by a square function.

Table 7. Listing of $K'_{meas}$ (K, Na) and $C^{v}_{HCl}$ values for vapor-silicate melt experiments performed at 800°C and 100 MPa.

| Sample | $K'_{meas}$ (K, Na) | $C^{v}_{HCl}$ (wt%) |
|---|---|---|
| 36 | 0.89 ± 0.13 | $1.4 \pm 0.3 \times 10^{-1}$ |
| 37 | 0.73 ± 0.08 | $1.0 \pm 0.8 \times 10^{-1}$ |
| 38 | 0.61 ± 0.08 | $2.1 \pm 0.3 \times 10^{-1}$ |
| 39 | 0.70 ± 0.10 | $1.1 \pm 0.2 \times 10^{-1}$ |

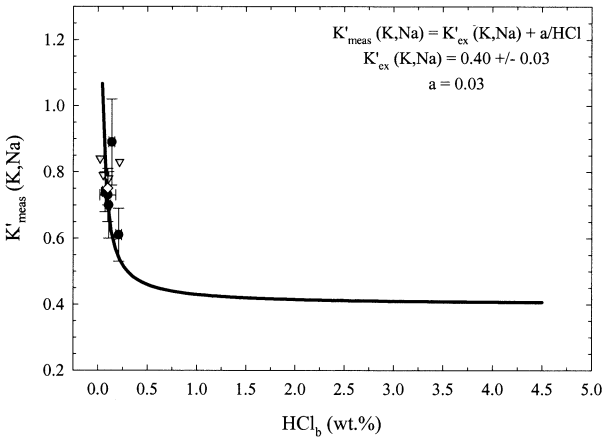


Fig. 5. Comparison of the model for brine–melt exchange of potassium and sodium as a function of HCl, outlined in Fig. 2, vs. the vapor experiments performed in this study (black circles), Holland (1972) (black square), Shinohara (1987) (gray diamond), and select experiments from Williams et al. (1997) (gray triangles). The close agreement indicates that the brine–melt model may be applicable to vapor-melt systems as well. All error bars are $1\sigma$.

To date, much of the data for metal partitioning between a volatile phase and melt are presented in the literature as metal–sodium exchange equilibria (i.e., $K_{Cu,Na}$ for the exchange of copper and sodium; cf. Candela and Piccoli, 1995, 1998). The variation in $K'_{meas}$ (K, Na) observed in this study implies that the treatment of metal partitioning between a volatile phase and melt as metal–alkali exchange equilibria is complicated by a dependence of sodium partitioning between melt and volatile phases on the fugacity of HCl, which is controlled ultimately by factors such as the fugacity of water and ASI. This may explain partially discrepancies in metal–alkali exchange equilibria presented in the literature. Therefore, metal–alkali exchange cannot be described fully without at least controlling or measuring melt ASI, or aqueous HCl.

Although the model of Candela (1990) relates melt composition to that of a coexisting MVP, the inability of the model to account for melts with an ASI $\leq 1$ poses problems because a portion of ore deposits are associated with peralkaline melts (Meinert, 1998). To modestly relax this restriction in melt aluminosity, a thermodynamic model was developed herein that allows for the calculation of HCl concentrations in brines based on $NaOH^m/\Sigma Na^m$ values in subaluminous melts and the $H_2O$ fugacity of the system. The apparent equilibrium constant, K' (NaOH), is $7.7(\pm 0.8) \times 10^4$; $1\sigma$ (where fugacity is in bars, and the concentrations are in wt%), for the equilibrium denoted by Eqn. 15 for experiments in the brine–melt system at 800°C and 100 MPa. Therefore, $C^{b}_{HCl}$ can be calculated if the other variables are known.

For subaluminous rocks, the $H_2O$ fugacity can be estimated by using the fugacity of pure water at the prevailing pressure

and temperature as a maximum value. The total sodium content of the melt can be obtained through analyses of the sodium content of rocks thought to closely approximate the composition of the melt at MVP saturation. The calculated NaOH component may represent both Na and OH that is not a part of the network forming structure, and of undetermined degree of ionization, or dissociation. The hypothesized functional relationship among the model concentrations of $NaOH^m$, quasichemical OH in the melt, molecular water ($H_2O^m$), $NaAlO_2^m$ (i.e., Na in its charge-balancing role), $HAlO_2^m$ (i.e., OH coordinated to the network, acting in a charge balancing role), $H_2O$ in the melt, and NaCl and HCl in the brine, can be elucidated by

$$NaOH^m + HCl^b = NaCl^b + H_2O^b \quad (26)$$

$$NaAlO_2^m + HCl^b = NaCl^b + HAlO_2^m, \quad (27)$$

which together define the linearly dependent equilibrium

$$NaAlO_2^m + H_2O^m = NaOH^m + HAlO_2^m \quad (28)$$

presented as Eqn. 12 and is an explicit version of Eqn. 24. The concentration of molecular water in the melt is controlled by the simple equilibrium

$$H_2O^b = H_2O^m \quad (29)$$

(Silver and Stolper, 1985; Holloway and Blank, 1994). The mass balance constraints

$$\Sigma Na^m = NaOH^m + NaAlO_2^m \quad (30)$$

and

$$\Sigma H^m = NaOH^m + HAlO_2^m + 2\ H_2O^m \quad (31)$$

define further the relationships among the variables. For a vapor-undersaturated brine with an activity of water = 0.6 (on an activity scale where unity indicates vapor saturation), data presented in Holloway and Blank (1994) suggest that at 850°C and 100 MPa, the concentrations of molecular and total water are given by 1.2 and 3.0 wt%, respectively. By using the equilibrium constant from Eqn. 26 recast in mol/kg melt, and the equilibrium constant for Eqn. 27 (from Williams et al., 1997) of ~0.6, an equilibrium constant for Eqn. 28 of $1.8 \times 10^{-6}$ can be computed (mol/kg). Combining this with the expressions for sodium and hydrogen balance in the melt, yields, for a concentration of 0.65 mol $NaAlO_2$ complexes per kilogram of melt (an equivalent of 5.3 wt% $NaAlO_2$ or 2 wt% $Na_2O$) and a fugacity of water of ~600 bars, two possible values for the concentration of NaOH in the melt: $5.8 \times 10^{-4}$ or 0.88 mol/kg can be calculated. However, the calculated HCl concentration in the brine for the low value of NaOH corresponds to an unrealistic brine HCl concentration (~60 wt%). The higher NaOH concentration corresponds to a lower HCl concentration in the brine of ~0.02 wt%. This implies that $HAlO_2$ has a concentration of $1.6 \times 10^{-3}$ mol/kg and therefore indicate that hydrogen in the melt is dominated by molecular water and hydroxyl groups. We calculated model NaOH and $NaAlO_2$ proportions of 0.58 and 0.42, respectively. Figure 6 shows further that higher concentrations of HCl in the brine lead to slightly higher concentrations of Cl in the melt. The increase in melt Cl was not the result of increased activity of alkali chlorides. Either some HCl monomer is present in the melt, or reduction of the NaOH component allows for less steric hindrance in these highly polymerized melts, and this probably results in a lower excess chemical potential for NaCl and KCl.

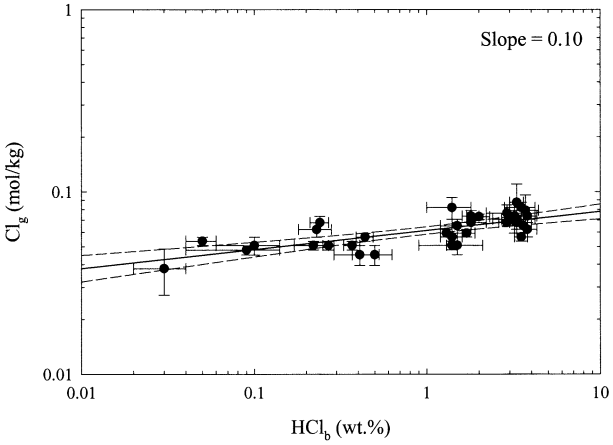


Fig. 6. The concentration of chloride in the glass (quenched melt) in this study was found to be affected slightly by the HCl concentration of a coexisting brine. The solid line is a line of linear regression, slope = 0.1, and the dashed line is the 95% confidence interval.

## 7. CONCLUSIONS

Experiments were performed in brine–melt and vapor–melt systems at 800°C and 100 MPa to evaluate the exchange of components between the MVP and silicate melt as a function of the HCl concentration of the MVP. $C^m_{Na}$ was found to be lowered relative to $C^m_K$ as $C^b_{HCl}$ was increased, and as a consequence, the $K'_{meas}$ (K, Na) decreased as well. $K'_{meas}$ (K, Na) decreased from 1.0 to 0.40 ± 0.03 ($1\sigma$) at $C^b_{KCl}$ of $3.0 \times 10^{-2}$ and 4.0 wt%, respectively. We hypothesize that this decrease corresponds to a decreasing role of the model sodium hydroxide component. In this model, higher values of $K'_{meas}$ (K, Na) correspond to the exchange of alkalis between brine and melt with both aluminate and hydroxide components whereas the lower limit of corresponds to the exchange of alkalis between brine and aluminate component in the melt alone. $K'_{meas}$ (K, Na) was found to be variable and a complex function of total sodium in the melt, modeled NaOH in the melt, water fugacity of the system and chloride to water ratio. The results suggest the hypothesis that (1) melt hydration increased the activity of NaOH and $HAlO_2$ components of the melt; (2) HCl in the brine reacted with the sodium hydroxide component of the melt to produce $H_2O$ and NaCl; and (3) the NaOH component of the melt is more likely to exercise control over MVP acidity than the KOH component of the melt. Therefore, previous treatments of metal–alkali exchange by a single metal–alkali equilibrium that ignored the affect of acidity may not depict the system fully; thus, multiple equilibria must be used to describe metal–alkali exchange.

The main control on model $NaOH^m/\Sigma Na^m$ in subaluminous melts is the fugacity of $H_2O$ in the system, with increasing $f^{sys}_{H_2O}$ increasing model $NaOH^m/\Sigma Na^m$. Although increases in $f^{sys}_{H_2O}$ in-

crease $NaOH^m/\Sigma Na^m$ in subaluminous melts, the HCl/NaCl of an exsolving MVP will increase at a greater rate because the two ratios are related by a square function. Increasing the ASI of the melt further increases the activity of the $HAlO_2$ component, which, by Le Châtelier's law, increases HCl in the volatile phases. Grounded on the observed relationship between the $C_{HCl}^{MVP}$ and $K'_{meas}$ (K, Na), a model was developed that allows for the calculation of $C_{HCl}^{MVP}$ predicated on the model NaOH/ΣNa value of the melt. Melts with an initially low model NaOH/ΣNa will produce an MVP with high HCl because the model NaOH component in the melt acts as a base that can decrease the acidity of the exsolved MVP. The model presented above demonstrates that melt composition has a great control over the composition of an exsolving MVP. Application of this model allows for a more complete understanding of the relationship among alteration assemblages, ore deposition, and the composition of the causative silicate melt.

*Acknowledgments*—Support for this project was provided by the National Science Foundation (EAR 9506631 [P.A.C. and P.M.P.]; EAR 9805313 [P.A.C. and P.M.P.]; EAR 9810244 [P.A.C., P.M.P., and others]), Sigma Xi Grants in Aid of Research (M.R.F.), and BHP Student Research Grant from the Society of Economic Geologists (M.R.F.). GCA reviews by David London, I-Ming Chou, and D. B. Dingwell improved the manuscript of this article considerably and are greatly appreciated.

*Associate editor:* D. B. Dingwell

## REFERENCES

Anderko A. and Pitzer K. S. (1993a) Equation-of-state representation of phase equilibria and volumetric properties of the system NaCl-$H_2O$ above 573 K. *Geochim. Cosmochim. Acta* **57,** 1657–1680.

Anderko A. and Pitzer K. S. (1993b) Phase Equilibria and volumetric properties of the system KCl-$H_2O$ and NaCl-KCl-$H_2O$ above 573 K: Equation of state and representation. *Geochim. Cosmochim. Acta* **57,** 4885–4897.

Candela P. A. (1990) Theoretical constraints on the chemistry of the magmatic aqueous phase. Special Paper 246, pp. 11–20. Geological Society of America.

Candela P. A. and Holland H. D. (1984) The partitioning of copper and molybdenum between silicate melts and aqueous fluids. *Geochim. Cosmochim. Acta* **48,** 373–380.

Candela P. A. and Piccoli P. M. (1995) Model ore–metal partitioning from melts into vapor and vapor/melt mixtures. In *Magmas, Fluids, and Ore Deposits*, (ed. J. F. H. Thompson), pp. 101–127. Mineralogical Association of Canada 23.

Candela P. A. and Piccoli P. M. (1998) Magmatic contributions to hydrothermal ore deposits; an algorithm (MVPart) for calculating the composition of the magmatic volatile phase. In *Techniques in Hydrothermal Ore Deposits Geology* (eds. J. P. Richards and P. B. Larson), pp. 97–108. Reviews in Economic Geology.

Chou I.-M. (1987) Phase relations in the system NaCl-KCl-$H_2O$; III, Solubilities of halite in vapor-saturated liquids above 445°C and redetermination of phase equilibrium properties in the system NaCl-$H_2O$ to 1000°C and 1500 bars. *Geochim. Cosmochim. Acta* **51,** 1965–1975.

Chou I., Sterner S. M., and Pitzer K. S. (1992) Phase relations in the system NaCl-KCl-$H_2O$: IV. Differential thermal analysis of the sylvite liquidus in the KCl-$H_2O$ binary, the liquidus in the NaCl-KCl-$H_2O$ ternary, and the solidus in the NaCl-KCl binary to 2 kb pressure, and a summary of experimental data for thermodynamic-PTX analysis of solid-liquid equilibria at elevated P-T conditions. *Geochim. Cosmochim. Acta* **56,** 2281–2293.

Frank M. R., Candela P. A., and Piccoli P. M. (1998) K–feldspar–muscovite–andalusite–quartz–brine phase equilibria: An experimental study at 25 to 60 MPa and 400 to 550°C. *Geochim. Cosmochim. Acta* **62,** 3717–3727.

Frank M. R., Candela P. A., Piccoli P. M., and Glascock M. D. (2002) Gold solubility speciation and partitioning as a function of HCl in the brine–silicate melt–metallic gold system at 800°C and 100 MPa. *Geochim. Cosmochim. Acta* **66,** 3719–3732.

Gammon J. B., Borcsik M., and Holland H. D. (1969) Potassium–sodium ratios in aqueous solutions and coexisting silicate melts. *Science* **163,** 179–181.

Gammons C. H. and Williams-Jones A. E. (1995) Chemical mobility of gold in the porphyry–epithermal environment. *Econ. Geol.* **92,** 45–59.

Hemley J. J. (1959) Some mineralogical equilibria in the system $K_2O$-$Al_2O_3$-$SiO_2$-$H_2O$. *Am. J. Sci.* **257,** 241–270.

Hemley J. J. and Hunt J. P. (1992) Hydrothermal ore-forming processes in the light of studies in rock-buffered systems; II Some general geologic applications. *Econ. Geol.* **87,** 23–43.

Holland H. D. (1972) Granites, solutions, and base metal deposits. *Econ. Geol.* **67,** 281–301.

Holloway J. R. and Blank J. G. (1994) Application of experimental results to C-O-H species in natural melts. In *Volatiles in Magmas*, 30 (eds. M. R. Carroll and J. R. Holloway), pp. 187–230. Mineralogical Society of America.

Holtz F., Behrens H., Dingwell D. B., and Taylor R. P. (1992) Water solubility in aluminosilicate melts of haplogranite composition at 2 kbar. *Chem. Geol.* **96,** 289–302.

Holtz F., Behrens H., Dingwell D. B., and Johannes W. (1995) $H_2O$ solubility in haplogranitic melts; compositional pressure and temperature dependence. *Am. Mineral.* **80,** 94–108.

Kohn S. C., Dupree R., and Smith M. E. (1989) A multinuclear magnetic resonance study of the structure of hydrous albite glasses. *Geochim. Cosmochim. Acta* **53,** 2925–2935.

Kohn S. C., Dupree R., and Mortuza M. G. (1992) The interaction between water and aluminosilicate magmas. *Chem. Geol.* **96,** 399–409.

Kohn S. C., Smith M. E., Dupree R., Sykes D., and Kubicki J. D. (1994) Comment on a model for $H_2O$ solubility mechanisms in albite melts from infrared spectroscopy and molecular orbital calculations; discussion and reply. *Geochim. Cosmochim. Acta* **58,** 1377–1384.

Kohn S. C., Smith M. E., Dirken P. J., van-Eck E. R. H., Kentgens A. P. M., and Dupree R. (1998) Sodium environments in dry and hydrous albite glasses; improved $^{23}Na$ solid state NMR data and their implications for water dissolution mechanisms. *Geochim. Cosmochim. Acta* **62,** 79–87.

Meinert L. D. (1998) A review of skarns that contain gold. In *Mineralized Intrusion-Related Skarn Systems* (ed. D. R. Lentz), Mineralogical Association of Canada Short Course Handbook 26, pp. 359–414.

Mysen B. O. and Virgo D. (1986) Volatiles in silicate melts at high pressure and temperature. 1. Interaction between OH groups and $Si^{4+}$ $Al^{3+}$ $Ca^{2+}$ $Na^+$ and $H^+$. *Chem. Geol.* **57,** 303–331.

Mysen B. O. and Acton M. (1999) Water in $H_2O$-saturated magma–fluid systems; solubility behavior in $K_2O$-$Al_2O_3$-$SiO_2$-$H_2O$ to 2.0 GPa and 1300°C. *Geochim. Cosmochim. Acta* **63,** 3799–3815.

Mysen B. O. and Wheeler K. (2000) Alkali aluminosilicate-saturated aqueous fluids in the Earth's upper mantle. *Geochim. Cosmochim. Acta* **64,** 4243–4256.

Nowak M. and Behrens H. (1995) The speciation of water in haplogranitic glasses and melts determined by in situ near-infrared spectroscopy. *Geochim. Cosmochim. Acta* **59,** 3445–3450.

Pichavant M. (1981) An experimental study of the effect of Boron on a water saturated haplogranite at 1 kbar vapour pressure. *Contrib. Mineral. Petrol.* **76,** 430–439.

Schäfer B., Frischknecht R., Günther D., and Dingwell D. B. (1999) Determination of trace-element partitioning between fluid and melt using LA-ICP-MS analysis of synthetic fluid inclusions in glass. *Eur. J. Mineral.* **11,** 415–426.

Schmidt B. C., Holtz F., Scaillet B., and Pichavant M. (1997) The influence of $H_2O$-$H_2$ fluids and redox conditions on melting temperatures in the haplogranite system. *Contrib. Mineral. Petrol.* **126,** 386–400.

Schmidt B. C., Riemer T., Kohn S. C., Holtz F., and Dupree R. (2001) Structural implications of water dissolution in haplogranitic glasses from NMR spectroscopy; influence of total water content and mixed alkali effect. *Geochim. Cosmochim. Acta* **65,** 2949–2964.

Shand S. J. (1951) *Eruptive Rocks: Their Genesis, Composition, Classification, and Their Relation to Ore-Deposits*. 4th ed. Hafner.

Shen A. and Keppler H. (1995) Infrared spectroscopy of hydrous silicate melts to 1000 degrees C and 10 kbar; direct observation of $H_2O$ speciation in a diamond-anvil cell. *Am. Mineral.* **80,** 1335–1338.

Shinohara H. (1987) Partitioning of chlorine compounds in the system silicate melt and hydrothermal solutions. Ph.D. dissertation. Tokyo Institute of Technology.

Silver L. and Stolper E. (1985) A thermodynamic model for hydrous silicate melts. *J. Geol.* **93,** 161–178.

Stolper E. M. (1982) The speciation of water in silicate melts. *Geochim. Cosmochim. Acta* **46,** 2295–2309.

Student J. J. and Bodnar R. J. (1999) Synthetic fluid inclusions XIV: Coexisting silicate melt and aqueous fluid inclusions in the haplogranite-$H_2O$-NaCl-KCl system. *J. Petrol.* **40,** 1509–1525.

Sverjensky D. A., Hemley J. J., and D'Angelo W. M. (1991) Thermodynamic assessment of hydrothermal alkali feldspar–mica–aluminosilicate equilibria. *Geochim. Cosmochim. Acta* **55,** 989–1004.

Tuttle O. F. and Bowen N. L. (1958) Origin of granite in the light of experimental studies in the system $NaAlSi_3O_8$-$KAlSi_3O_8$-$SiO_2$-$H_2O$. *Geol. Soc. Am. Mem.* **74**.

Webster J. D. and Holloway J. R. (1988) Experimental constraints on the partitioning of C1 between topaz rhyolite melt and $H_2O$ and $H_2O$ + $CO_2$ fluids; new implications for granitic differentiation and ore deposition. *Geochim. Cosmochim. Acta* **52,** 2091–2105.

Webster J. D., Holloway J. R., and Hervig R. L. (1989) Partitioning of lithophile trace elements between $H_2O$ and $H_2O$ + $CO_2$ fluids and topaz rhyolite melt. *Econ. Geol.* **84,** 116–134.

Williams T. J., Candela P. A., and Piccoli P. M. (1995) The partitioning of copper between silicate melts and two-phase aqueous fluids; an experimental investigation at 1 kbar, 800°C and 0.5 kbar, 850°C. *Contrib. Mineral. Petrol.* **121,** 388–399.

Williams T. J., Candela P. A., and Piccoli P. M. (1997) Hydrogen–alkali exchange between silicate melts and two-phase aqueous mixtures: An experimental investigation. *Contrib. Mineral Petrol.* **128,** 114–126.

Yamashita S. (1999) Experimental study of the effect of temperature on water solubility in natural rhyolite melt to 100 MPa. *J. Petrol.* **40,** 1497–1507.